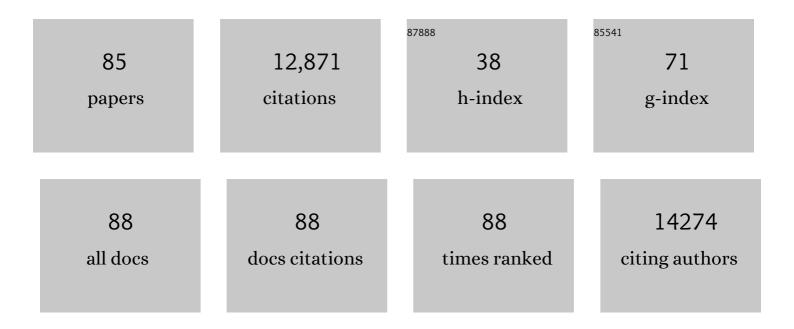
List of Publications by Year in descending order

Source: https://exaly.com/author-pdf/6937618/publications.pdf Version: 2024-02-01



#	Article	IF	CITATIONS
1	Low trap-state density and long carrier diffusion in organolead trihalide perovskite single crystals. Science, 2015, 347, 519-522.	12.6	4,156
2	High-quality bulk hybrid perovskite single crystals within minutes by inverse temperature crystallization. Nature Communications, 2015, 6, 7586.	12.8	1,478
3	Formamidinium Lead Halide Perovskite Crystals with Unprecedented Long Carrier Dynamics and Diffusion Length. ACS Energy Letters, 2016, 1, 32-37.	17.4	752
4	CH ₃ NH ₃ PbCl ₃ Single Crystals: Inverse Temperature Crystallization and Visible-Blind UV-Photodetector. Journal of Physical Chemistry Letters, 2015, 6, 3781-3786.	4.6	636
5	Air-Stable Surface-Passivated Perovskite Quantum Dots for Ultra-Robust, Single- and Two-Photon-Induced Amplified Spontaneous Emission. Journal of Physical Chemistry Letters, 2015, 6, 5027-5033.	4.6	466
6	Heterovalent Dopant Incorporation for Bandgap and Type Engineering of Perovskite Crystals. Journal of Physical Chemistry Letters, 2016, 7, 295-301.	4.6	332
7	Zero-Dimensional Cs ₄ PbBr ₆ Perovskite Nanocrystals. Journal of Physical Chemistry Letters, 2017, 8, 961-965.	4.6	299
8	Solutionâ€Grown Monocrystalline Hybrid Perovskite Films for Holeâ€Transporterâ€Free Solar Cells. Advanced Materials, 2016, 28, 3383-3390.	21.0	298
9	Perovskite Photodetectors Operating in Both Narrowband and Broadband Regimes. Advanced Materials, 2016, 28, 8144-8149.	21.0	260
10	Intrinsic efficiency limits in low-bandgap non-fullerene acceptor organic solar cells. Nature Materials, 2021, 20, 378-384.	27.5	257
11	Perovskite Oxide SrTiO ₃ as an Efficient Electron Transporter for Hybrid Perovskite Solar Cells. Journal of Physical Chemistry C, 2014, 118, 28494-28501.	3.1	251
12	Ultralow Self-Doping in Two-dimensional Hybrid Perovskite Single Crystals. Nano Letters, 2017, 17, 4759-4767.	9.1	251
13	Giant Photoluminescence Enhancement in CsPbCl ₃ Perovskite Nanocrystals by Simultaneous Dual-Surface Passivation. ACS Energy Letters, 2018, 3, 2301-2307.	17.4	244
14	Inside Perovskites: Quantum Luminescence from Bulk Cs ₄ PbBr ₆ Single Crystals. Chemistry of Materials, 2017, 29, 7108-7113.	6.7	200
15	Ultrathin Cu ₂ O as an efficient inorganic hole transporting material for perovskite solar cells. Nanoscale, 2016, 8, 6173-6179.	5.6	191
16	Engineering of CH ₃ NH ₃ PbI ₃ Perovskite Crystals by Alloying Large Organic Cations for Enhanced Thermal Stability and Transport Properties. Angewandte Chemie - International Edition, 2016, 55, 10686-10690.	13.8	152
17	Optoelectronic and photovoltaic properties of the air-stable organohalide semiconductor (CH ₃ NH ₃) ₃ Bi ₂ I ₉ . Journal of Materials Chemistry A, 2016, 4, 12504-12515.	10.3	151
18	Amorphous Tin Oxide as a Low-Temperature-Processed Electron-Transport Layer for Organic and Hybrid Perovskite Solar Cells. ACS Applied Materials & Interfaces, 2017, 9, 11828-11836.	8.0	145

#	Article	IF	CITATIONS
19	Surface Restructuring of Hybrid Perovskite Crystals. ACS Energy Letters, 2016, 1, 1119-1126.	17.4	140
20	Harnessing structural darkness in the visible and infrared wavelengths for a new source of light. Nature Nanotechnology, 2016, 11, 60-66.	31.5	125
21	Ultrahigh Carrier Mobility Achieved in Photoresponsive Hybrid Perovskite Films via Coupling with Singleâ€Walled Carbon Nanotubes. Advanced Materials, 2017, 29, 1602432.	21.0	106
22	Fast Crystallization and Improved Stability of Perovskite Solar Cells with Zn ₂ SnO ₄ Electron Transporting Layer: Interface Matters. ACS Applied Materials & Interfaces, 2015, 7, 28404-28411.	8.0	103
23	Pyridine-Induced Dimensionality Change in Hybrid Perovskite Nanocrystals. Chemistry of Materials, 2017, 29, 4393-4400.	6.7	100
24	Facile Synthesis and High Performance of a New Carbazole-Based Hole-Transporting Material for Hybrid Perovskite Solar Cells. ACS Photonics, 2015, 2, 849-855.	6.6	99
25	Quantum Confinement-Tunable Ultrafast Charge Transfer at the PbS Quantum Dot and Phenyl-C ₆₁ -butyric Acid Methyl Ester Interface. Journal of the American Chemical Society, 2014, 136, 6952-6959.	13.7	97
26	The Surface of Hybrid Perovskite Crystals: A Boon or Bane. ACS Energy Letters, 2017, 2, 846-856.	17.4	91
27	Carrier dynamics of a visible-light-responsive Ta ₃ N ₅ photoanode for water oxidation. Physical Chemistry Chemical Physics, 2015, 17, 2670-2677.	2.8	85
28	Ultralong Radiative States in Hybrid Perovskite Crystals: Compositions for Submillimeter Diffusion Lengths. Journal of Physical Chemistry Letters, 2017, 8, 4386-4390.	4.6	83
29	Generation of Multiple Excitons in Ag ₂ S Quantum Dots: Single High-Energy versus Multiple-Photon Excitation. Journal of Physical Chemistry Letters, 2014, 5, 659-665.	4.6	81
30	Water-Induced Dimensionality Reduction in Metal-Halide Perovskites. Journal of Physical Chemistry C, 2018, 122, 14128-14134.	3.1	78
31	Ultrafast electron injection at the cationic porphyrin–graphene interface assisted by molecular flattening. Chemical Communications, 2014, 50, 10452.	4.1	68
32	Ligand-Free Nanocrystals of Highly Emissive Cs ₄ PbBr ₆ Perovskite. Journal of Physical Chemistry C, 2018, 122, 6493-6498.	3.1	63
33	Double Charged Surface Layers in Lead Halide Perovskite Crystals. Nano Letters, 2017, 17, 2021-2027.	9.1	60
34	Triplet excited state properties in variable gap π-conjugated donor–acceptor–donor chromophores. Chemical Science, 2016, 7, 3621-3631.	7.4	59
35	Study on the use of optical coherence tomography in measurements of paper properties. Measurement Science and Technology, 2005, 16, 1131-1137.	2.6	58
36	Real-Time Observation of Ultrafast Intraband Relaxation and Exciton Multiplication in PbS Quantum Dots. ACS Photonics, 2014, 1, 285-292.	6.6	54

#	Article	IF	CITATIONS
37	Optical coherence tomography as an accurate inspection and quality evaluation technique in paper industry. Optical Review, 2010, 17, 218-222.	2.0	46
38	Solvent-Dependent Excited-State Hydrogen Transfer and Intersystem Crossing in 2-(2′-Hydroxyphenyl)-Benzothiazole. Journal of Physical Chemistry B, 2015, 119, 2596-2603.	2.6	40
39	Optical coherence tomography as a method of quality inspection for printed electronics products. Optical Review, 2010, 17, 257-262.	2.0	39
40	Temperature-Induced Lattice Relaxation of Perovskite Crystal Enhances Optoelectronic Properties and Solar Cell Performance. Journal of Physical Chemistry Letters, 2017, 8, 137-143.	4.6	39
41	Direct Femtosecond Observation of Charge Carrier Recombination in Ternary Semiconductor Nanocrystals: The Effect of Composition and Shelling. Journal of Physical Chemistry C, 2015, 119, 3439-3446.	3.1	38
42	Photophysics of Organometallic Platinum(II) Derivatives of the Diketopyrrolopyrrole Chromophore. Journal of Physical Chemistry A, 2014, 118, 11735-11743.	2.5	36
43	Impact of Metal Ions in Porphyrinâ€Based Applied Materials for Visibleâ€Light Photocatalysis: Key Information from Ultrafast Electronic Spectroscopy. Chemistry - A European Journal, 2014, 20, 10475-10483.	3.3	36
44	Photoinduced triplet-state electron transfer of platinum porphyrin: a one-step direct method for sensing iodide with an unprecedented detection limit. Journal of Materials Chemistry A, 2015, 3, 6733-6738.	10.3	33
45	Ultrafast Carrier Trapping of a Metal-Doped Titanium Dioxide Semiconductor Revealed by Femtosecond Transient Absorption Spectroscopy. ACS Applied Materials & Interfaces, 2014, 6, 10022-10027.	8.0	32
46	Detection of local specular gloss and surface roughness from black prints. Colloids and Surfaces A: Physicochemical and Engineering Aspects, 2007, 299, 101-108.	4.7	31
47	A Layerâ€byâ€Layer ZnO Nanoparticle–PbS Quantum Dot Selfâ€Assembly Platform for Ultrafast Interfacial Electron Injection. Small, 2015, 11, 112-118.	10.0	31
48	Online monitoring of printed electronics by Spectral-Domain Optical Coherence Tomography. Scientific Reports, 2013, 3, 1562.	3.3	28
49	Tuning Soluteâ€Redistribution Dynamics for Scalable Fabrication of Colloidal Quantumâ€Dot Optoelectronics. Advanced Materials, 2019, 31, e1805886.	21.0	28
50	Characterisation of optically cleared paper by optical coherence tomography. Quantum Electronics, 2006, 36, 181-187.	1.0	27
51	How Humidity and Light Exposure Change the Photophysics of Metal Halide Perovskite Solar Cells. Solar Rrl, 2020, 4, 2000382.	5.8	23
52	Ultra-high resolution optical coherence tomography for encapsulation quality inspection. Applied Physics B: Lasers and Optics, 2011, 105, 649-657.	2.2	22
53	Real-Space Mapping of Surface Trap States in CIGSe Nanocrystals Using 4D Electron Microscopy. Nano Letters, 2016, 16, 4417-4423.	9.1	22
54	Remarkable Fluorescence Enhancement versus Complex Formation of Cationic Porphyrins on the Surface of ZnO Nanoparticles. Journal of Physical Chemistry C, 2014, 118, 12154-12161.	3.1	19

#	Article	IF	CITATIONS
55	Real-time observation of ultrafast electron injection at graphene–Zn porphyrin interfaces. Physical Chemistry Chemical Physics, 2015, 17, 9015-9019.	2.8	19
56	Overcoming the Cutâ€Off Charge Transfer Bandgaps at the PbS Quantum Dot Interface. Advanced Functional Materials, 2015, 25, 7435-7441.	14.9	18
57	Tunable Photophysical Processes of Porphyrin Macrocycles on the Surface of ZnO Nanoparticles. Journal of Physical Chemistry C, 2015, 119, 2614-2621.	3.1	18
58	Engineering of CH ₃ NH ₃ PbI ₃ Perovskite Crystals by Alloying Large Organic Cations for Enhanced Thermal Stability and Transport Properties. Angewandte Chemie, 2016, 128, 10844-10848.	2.0	18
59	Glucose sensing in aqueous Intralipid suspension with an optical coherence tomography system: experiment and Monte Carlo simulation. , 2004, 5325, 164.		17
60	Bimolecular Excited-State Electron Transfer with Surprisingly Long-Lived Radical Ions. Journal of Physical Chemistry C, 2015, 119, 21896-21903.	3.1	16
61	Ultrafast Excited-State Dynamics of Diketopyrrolopyrrole (DPP)-Based Materials: Static versus Diffusion-Controlled Electron Transfer Process. Journal of Physical Chemistry C, 2015, 119, 15919-15925.	3.1	15
62	The impact of electrostatic interactions on ultrafast charge transfer at Ag ₂₉ nanoclusters–fullerene and CdTe quantum dots–fullerene interfaces. Journal of Materials Chemistry C, 2016, 4, 2894-2900.	5.5	12
63	<title>Noninvasive glucose sensing in scattering media using OCT, PAS, and TOF techniques</title> . , 2004, , .		11
64	Diffractive-optical-element-based glossmeter and low coherence interferometer in assessment of local surface quality of paper. Optical Engineering, 2006, 45, 043601.	1.0	10
65	Light-Harvesting Two-Photon-Absorbing Polymers. Macromolecules, 2020, 53, 6279-6287.	4.8	9
66	To what extent can charge localization influence electron injection efficiency at graphene–porphyrin interfaces?. Physical Chemistry Chemical Physics, 2015, 17, 14513-14517.	2.8	7
67	Optical coherence tomography of multilayer tissue based on the dynamical stochastic fringe processing. , 2003, , .		6
68	The Impact of Grain Alignment of the Electron Transporting Layer on the Performance of Inverted Bulk Heterojunction Solar Cells. Small, 2015, 11, 5272-5279.	10.0	6
69	<title>Optical coherence tomography in scattering material for industrial applications</title> ., 2001,		4
70	Optical coherence tomography evaluation of internal random structure of wood fiber tissue. , 2003, ,		4
71	Flow velocity profile measurement of scattering liquid using Doppler optical coherence tomography. , 2003, , .		4
72	Photoinduced energy and electron transfer in rubrene–benzoquinone and rubrene–porphyrin systems. Chemical Physics Letters, 2014, 616-617, 237-242.	2.6	4

#	Article	IF	CITATIONS
73	<title>Optical coherence tomography device for paper characterization</title> ., 2004, , .		2
74	Nd:YAG laser annealing investigation of screen-printed CIGS layer on PET: Layer annealing method for photovoltaic cell fabrication process. , 2014, , .		2
75	Real-time observation of intersystem crossing induced by charge recombination during bimolecular electron transfer reactions. Dyes and Pigments, 2017, 136, 881-886.	3.7	2
76	Optical coherence tomography evaluating the random tissues based on dynamical processing the stochastic low-coherence interference fringes. , 2003, , .		1
77	<title>Enhancing the OCT images by the low-coherence fringe envelope deconvolution method</title> . , 2004, 5486, 180.		1
78	Nonlinear dynamic filtering of logarithmically amplified fringe signals in optical coherence tomography applied to paper measurements. Optics and Spectroscopy (English Translation of Optika I) Tj ETQq0	0@&gBT /	Overlock 10
79	<title>Comparing low coherence interferometry with conventional methods of measuring paper roughness</title> . , 2007, , .		1
80	<title>Evaluation of a scattering liquid flow velocity profile using Doppler optical coherence
tomography and dynamic stochastic interference fringe processing</title> ., 2004, 5475, 66.		0
81	<title>Comparison of artificial neural network and multilinear regression analysis models in
estimation of pulp flow speed from low coherence Doppler flowmetry measurement data</title> . , 2007, , .		0
82	Quantum Dots: Overcoming the Cutâ€Off Charge Transfer Bandgaps at the PbS Quantum Dot Interface (Adv. Funct. Mater. 48/2015). Advanced Functional Materials, 2015, 25, 7548-7548.	14.9	0
83	Optical coherence tomography evaluating the random tissues based on dynamical processing the stochastic low-coherence interference fringes. , 2003, , .		0
84	<title>Neural network analysis of pulp flow speed in low coherence Doppler flowmetry measurement</title> . , 2007, , .		0
85	Blackbody metamaterial lasers. , 2015, , .		0